International Journal of Technology (2018) 6: 1178-1186
ISSN 2086-9614

SOLID ELECTROLYTES FOR LITHIUM BATTERIES

Xingxing Zhang[1], Jeffrey W. Fergus[1*]

[1]*Materials Research and Education Center, Auburn University, Auburn, Alabama 36849, USA*

(Received: May 2018 / Revised: July 2018 / Accepted: October 2018)

ABSTRACT

The use of solid electrolytes to produce an all-solid-state lithium battery is regarded as one promising alterative for improved safety. In this work, the researchers synthesized cubic garnet-type ceramic electrolyte $Li_{6.75}La_3Zr_{1.75}Ta_{0.25}O_{12}$ (LLZTO) via the coprecipitation method. For the characterization, the phase content was determined using X-ray diffraction (XRD), morphology was obtained by using a scanning electron microscope (SEM), and conductivity was measured by AC impedance spectroscopy using a frequency response analyzer. The results showed that the room temperature total conductivity and activation energies of LLZTO were 7.2×10^{-6} S/cm and 0.31–0.46 eV, respectively. Composite electrolytes were prepared by mixing LLZTO with a ceramic ($Li_{1.4}Al_{0.4}Ti_{1.6}(PO_4)$) (NASICON) or a polymer polyethylene oxide (PEO) with $LiClO_4$ salt. The LLZTO-NASICON composite showed a higher total conductivity of 1.2×10^{-5} S/cm and activation energies of 0.23–0.58 eV. Compared to LLZTO, the LLZTO-PEO($LiClO_4$) composite showed a similar room temperature total conductivity of 1.2×10^{-6} S/cm, but a higher activation energy of 0.59–0.85 eV.

Keywords: Garnet; Solid composite electrolyte; Solid electrolyte

1. INTRODUCTION

Lithium-ion batteries are widely used for energy storage in a variety of applications (Nitta et al., 2015). However, the commonly used organic carbonate liquid electrolytes have poor chemical stability, display high flammability, and can leak from the battery, which can create safety issues (Varzi et al., 2016). Using solid electrolytes instead of liquid electrolytes to produce an all-solid-state lithium battery is regarded as one promising way to improve safety (Reisch, 2017).

Solid-state electrolytes used in lithium-ion batteries can be divided into two categories: polymers and ceramics (Liu et al., 2018). The first category, solid polymer electrolytes (SPE), are formed by dissolving a lithium salt, such as $LiClO_4$, $LiBF_4$, or $LiN(CF_3SO_2)_2$, in a polymer host (Agrawal & Pandey, 2008; Zhang et al., 2017). The advantages of solid-state polymer electrolytes are ease of processing and mechanical flexibility. However, they exhibit poor electrochemical stability, low lithium ionic conductivity, and low mechanical strength (Ren et al., 2015; Zhao et al., 2016). The second category, ceramic electrolytes, have high chemical and electrochemical stability as well as high mechanical strength, but they are non-flexible. Much effort has been made toward the development of solid-state ceramic electrolytes, such as perovskite-type titanates (LLTO) (Kwon et al., 2017), NASICON-type (sodium super ionic conductor) oxide electrolytes (Morimoto et al., 2013), sulfide-type and garnet-type materials (Thangadurai et al., 2014; Manthiram et al., 2017).

*Corresponding author's email: ferguje@auburn.edu, Tel. +1 334-844-3405, Fax. +1 334-844-4487
Permalink/DOI: https://doi.org/10.14716/ijtech.v9i6.2502

The focus of this work was the garnet-type ceramic electrolyte $Li_7La_3Zr_2O_{12}$ (LLZO), as it has the most promising properties for solid electrolyte, such as high chemical stability and a high ionic conductivity of 3×10^{-4} S/cm at 25°C (Murugan et al., 2007). LLZO can form a tetragonal structure with low lithium-ion conductivity, approximately 2×10^{-6} S/cm (Awaka et al., 2009), so the elemental doping method was used to stabilize the more conductive cubic phase. In this work, tantalum doping was used to prepare the cubic phase LLZO. LLZO-based composites were also prepared in this work by combining a solid polymer electrolyte, PEO($LiClO_4$), or a NASICON-type material, $Li_{1.4}Al_{0.4}Ti_{1.6}(PO_4)$, with LLZO

2. METHODS

Tantalum-doped LLZO (LLZTO) was prepared by the coprecipitation method. Powders of LiOH (Alfa, anhydrous, 98%), $La(OH)_3$ (Alfa, 99.95% REO), $ZrOCl_2\cdot8H_2O$ (Alfa, 98%), Ta_2O_5 (Alfa, 99%, metal basis), nitric acid (Alfa, 67–70%) and NH_4OH (Alfa, 5.0N) were used as starting materials. Transparent solutions of LiOH and $La(OH)_3$ in HNO_3, and $ZrOCl_2\cdot8H_2O$ in deionized water were prepared first. Before mixing these two solutions, Ta_2O_5 powders were added into the nitric acid solution. NH_4OH was then added to the mixture to obtain precipitates. The precipitates were dried at 80°C for 48 hours first. With flowing room temperature air, the precipitates were heated to 700°C and held at 700°C for 2 hours. The dried powders were then ball milled with a planetary ball milling machine at 500 rpm for 4 hours. After drying at 80°C for 24 hours, the powders were cold-pressed into 10 mm diameter pellets. The pellets were covered with powders of the same composition as that of the pellets, put in alumina crucibles and then sintered at 1100°C for 16 hours in air with a heating rate of 1°C/min.

To obtain LLZTO-PEO($LiClO_4$) composites, a PEO($LiClO_4$) solution with a molar ratio of ethylene oxide segments to lithium ions of EO/Li=10 was first prepared. Appropriate amounts of PEO (Alfa, M.W. 100,000) and $LiClO_4$ (Alfa, anhydrous, 99%) were dissolved in acetonitrile (Alfa, 99%) and mixed in a magnetic stirrer until a transparent solution was obtained. The LLZTO pellets were sufficiently immersed in a PEO($LiClO_4$) solution and dried in vacuum oven at 50°C for 72 hours.

To prepare LLZTO-NASICON ($Li_{1.4}Al_{0.4}Ti_{1.6}(PO_4)$) composites, NASICON pellets were prepared separately by the coprecipitation method. Powders of $CH_3COOLi\cdot2H_2O$ (Sigma, 99.8%) and $Al(NO)_3$ (Sigma, ≥98%) were dissolved in deionized water to form a clear solution. $Ti[OCH(CH_3)_2]_4$ (Sigma, 98%) and $NH_4H_2PO_4$ (Sigma, ≥98%) were then added into this clear solution drop by drop to form precipitates. With flowing room temperature air, precipitates were heated to 350°C and held at 350°C for 2 hours and then heated to 800°C and held at 800°C for 30 minutes. The powders obtained were then cold pressed into 12.5 mm diameter pellets and sintered at 900°C for 6 hours. LLZTO powders, which were sintered at 700°C only and 10 wt% NASICON powders, which were obtained by grinding the NASICON pellets, were ball milled at 200 rpm for 3 hours and then cold pressed into 10 mm diameter pellets and sintered at 1100℃ for 16 hours.

For the characterization, the phase content was determined at room temperature using X-ray diffraction (XRD) with a Bruker D8 diffractometer with Cu X-ray source at 40 mA and 40 kV. Morphology was obtained by using a JEOL JSM-7000F scanning electron microscope (SEM). Conductivity was measured by AC impedance spectroscopy using a frequency response analyzer (Solartron 1260, USA) in the frequency range of 0.1 Hz–15 MHz with an amplitude of 50 mV. The silver electrodes were synthesized by coating silver paste on both sides of the pellet and curing at room temperature for 1 hour. The impedance spectra were fit to equivalent circuit models using ZView software.

3. RESULTS AND DISCUSSION

3.1. X-Ray Diffraction, Morphology and Electrochemical Impedance Spectroscopy of LLZTO

The XRD patterns of $Li_{6.75}La_3Zr_{1.75}Ta_{0.25}O_{12}$ sintered at 1100°C for 16 hours and standard diffraction spectrum of $Li_5La_3Nb_2O_{12}$ (PDF 45-0109) in Figure 1 show that LLZO with 0.25 mol% Ta has the pure cubic phase.

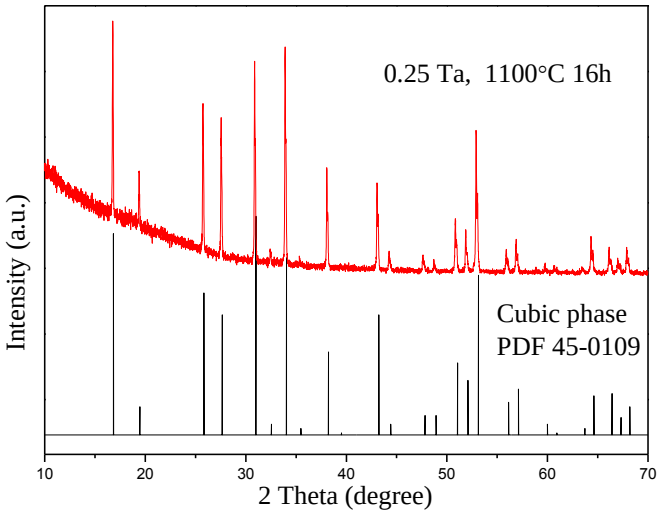

Figure 1 XRD pattern of $Li_{6.75}La_3Zr_{1.75}Ta_{0.25}O_{12}$

Figure 2 shows the measured conductivity of LLZTO. As shown in the typical Nyquist plot for a LLZTO pellet at room temperature in Figure 2a, the spectra were fit to an equivalent circuit of $(R_{HF}CPE_{HF})(R_{LF}CPE_{LF})(CPE_E)$, where R and CPE are the resistance and the constant phase element, respectively. The total resistance (R_{TOTAL}) can be calculated as the sum of high frequency (HF) and low frequency (LF) contributions (i.e. $R_{HF} + R_{LF}$). The room temperature total ionic conductivity of the LLZTO sample is 7.24×10^{-6} S/cm. The activation energy determined from the slope of the ln (σT) versus 1000/T plot is 0.31 eV for the high frequency contribution and 0.46 eV for the low frequency contribution.

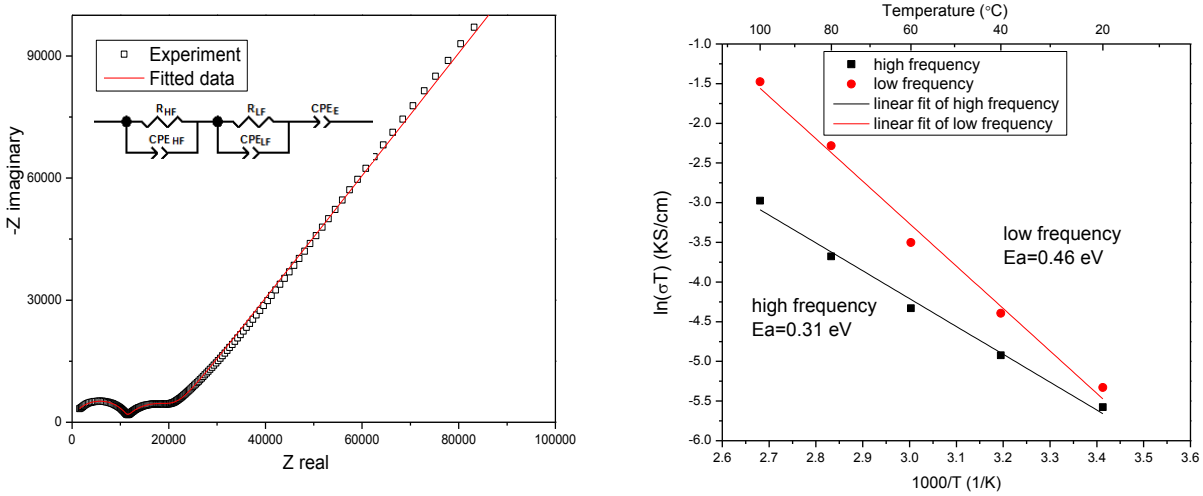

(a) room temperature impedance spectra (b) Arrhenius plot

Figure 2 Ionic conductivity data of $Li_{6.75}La_3Zr_{1.75}Ta_{0.25}O_{12}$

The total ionic conductivity for Ta-doped LLZO of 7.24×10^{-6} S/cm is two orders of magnitude lower than the reported ionic conductivity of 8.7×10^{-4} S/cm, which has a relative density of ~96-98% (Allen et al., 2012). The relative density of LLZTO obtained in this work is around 80% as measured by the Archimedes method. The SEM images of a cross-sectional area of LLZTO in Figure 3 show that there are many connected pores, which also indicates a low relative density. This low density may contribute to this low ionic conductivity, but the large difference in magnitude indicates that there may be an additional effect, such as a highly resistive phase at the interface between particles.

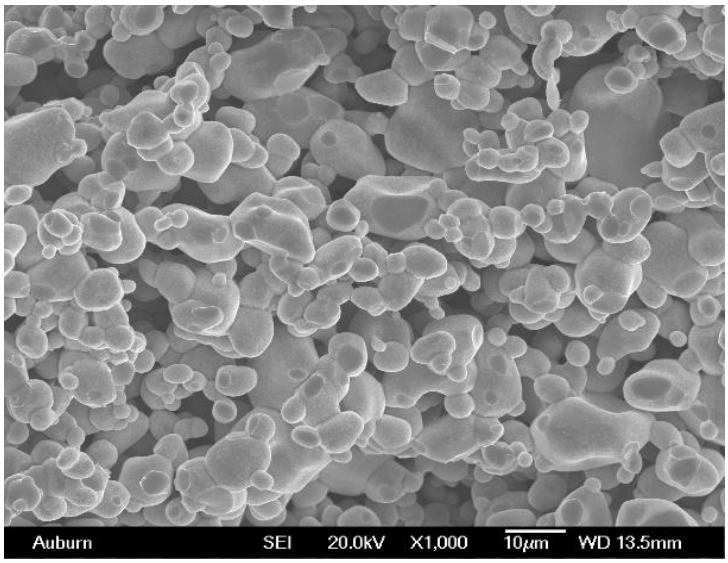

(a)

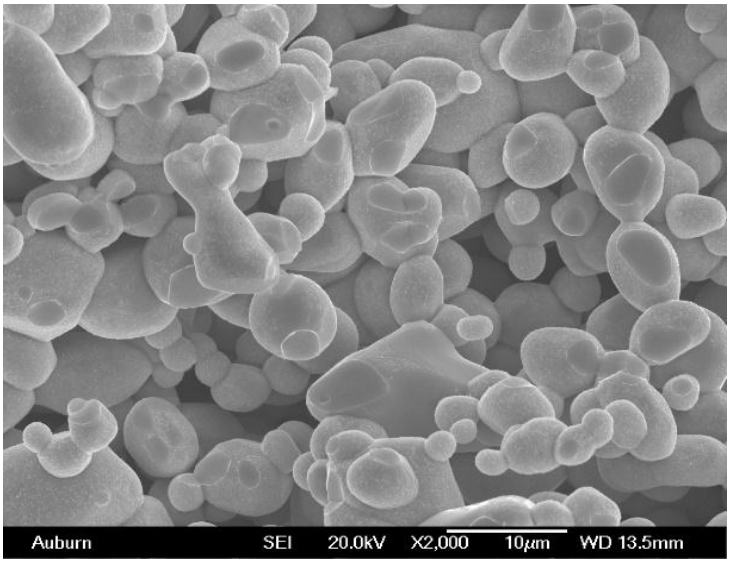

(b)

Figure 3 SEM images of the cross-section area of $Li_{6.75}La_3Zr_{1.75}Ta_{0.25}O_{12}$

3.2. Morphology and Electrochemical Impedance Spectroscopy of LLZTO-NASICON Composites

The SEM images of LLZTO-NASICON in Figure 4 show that LLZTO-NASICON composite samples have a similar porosity but a coarser structure as compared with LLZTO samples.

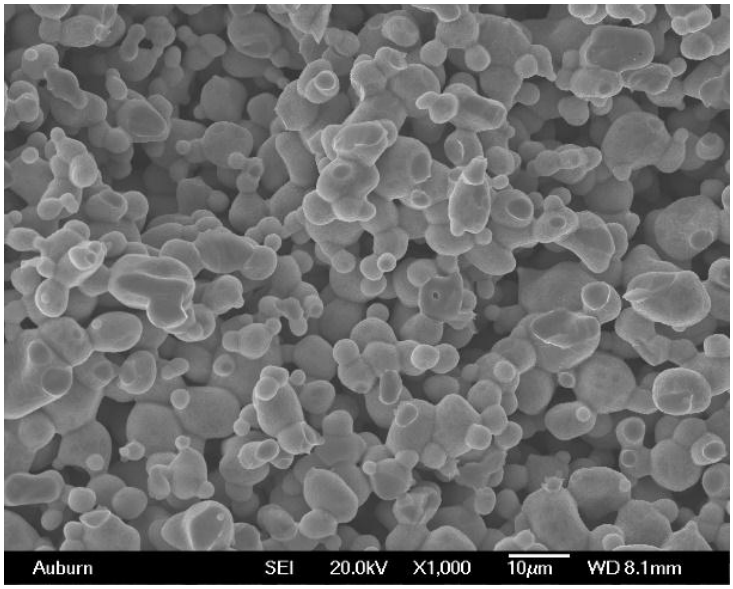

(a)

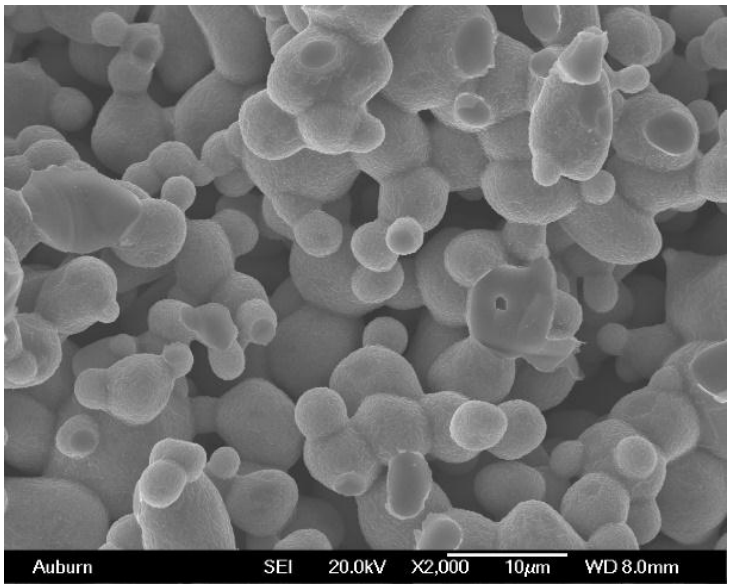

(b)

Figure 4 SEM images of the cross-section area of LLZTO-NASICON composite

An example of a Nyquist plot fit to the equivalent circuit described above and a summary of an Arrhenius plot for the LLZTO-NASICON composite are shown in Figure 5. At room temperature, the conductivity for the high frequency contribution is 1.66×10^{-5} S/cm, the low frequency contribution is 4.01×10^{-5} S/cm, and the total is 1.18×10^{-5} S/cm, which is higher than the total ionic conductivity of LLZTO, 7.24×10^{-6} S/cm. The activation energies were estimated to be 0.58 eV and 0.23 eV for high- and low-frequency contributions, respectively. When compared to LLZTO, LLZTO-NASICON composites show similar morphology but exhibit higher room temperature total conductivity.

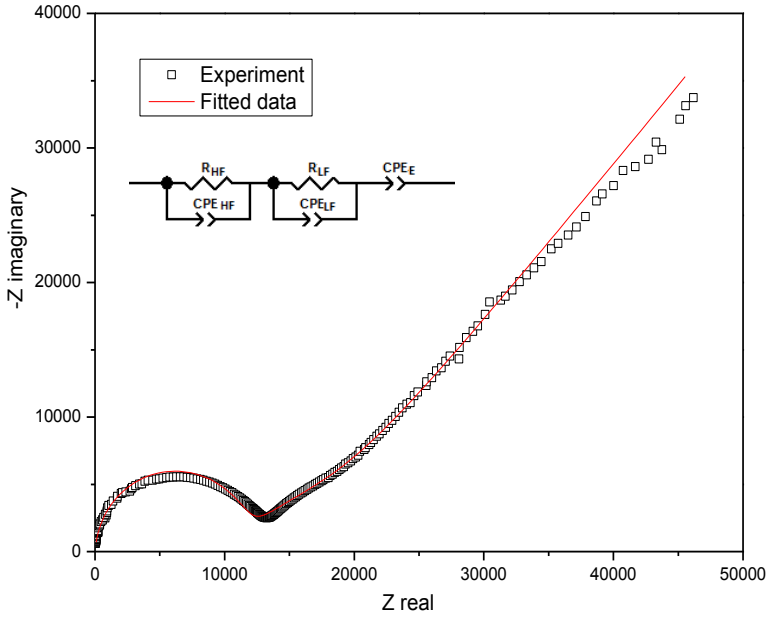

(a) room temperature impedance spectra

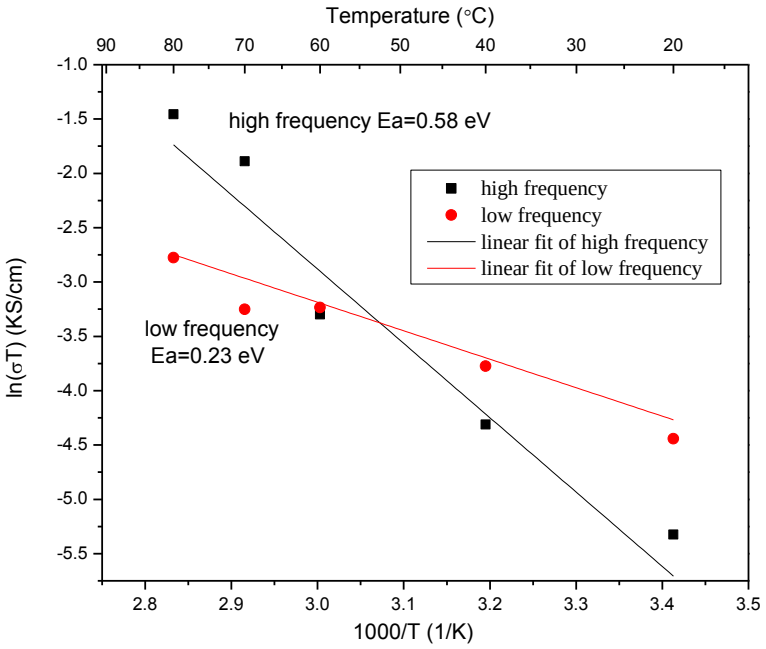

(b) Arrhenius plot

Figure 5 Ionic conductivity data LLZTO-NASICON composite

3.3. Morphology and Electrochemical Impedance Spectroscopy of LLZTO-PEO($LiClO_4$) Composites

SEM images of the cross-section area of the LLZTO-PEO($LiClO_4$) composite in Figure 6 show that the LLZTO-PEO($LiClO_4$) composite pellet is much denser than LLZTO (see Figure 3).

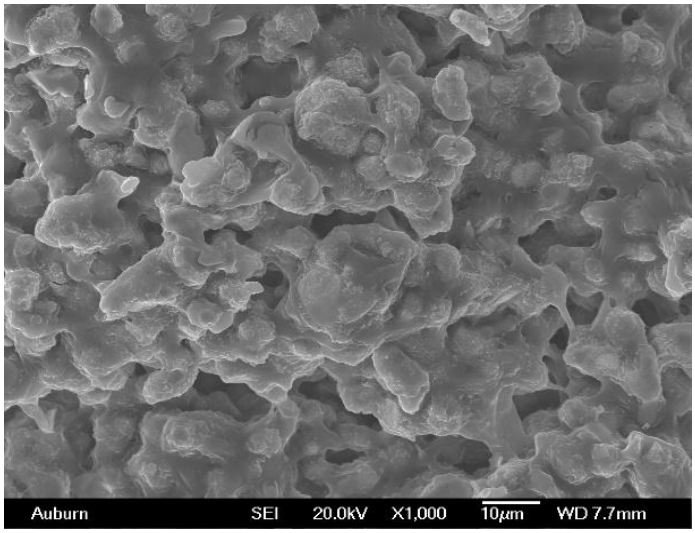

(a)

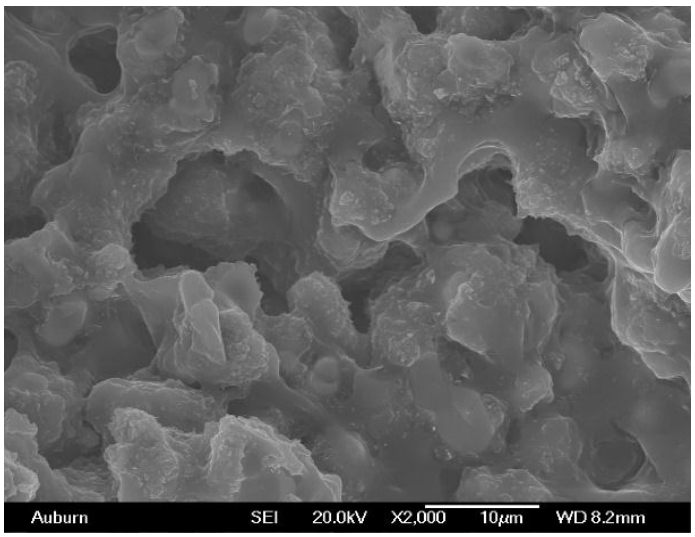

(b)

Figure 6 SEM images of the cross-section area of LLZTO-PEO($LiClO_4$) composite

An example of a Nyquist plot fit to the equivalent circuit model described above and a summary of an Arrhenius plot for the LLZTO-PEO($LiClO_4$) composite are shown in Figure 7. The room temperature total conductivity of 1.04×10^{-6} S/cm is smaller than that of the LLZTO pellet, which is 7.24×10^{-6} S/cm. The activation energies estimated from the slopes in the Arrhenius plot in Figure 7b are 0.85 eV and 0.59 eV for the high- and low-frequency contributions, respectively. The lower conductivity of LLZTO-PEO($LiClO_4$) relative to LLZTO may be due to the low conductivity of PEO($LiClO_4$) which is 1×10^{-7} S/cm (Agrawal & Pandey, 2008).

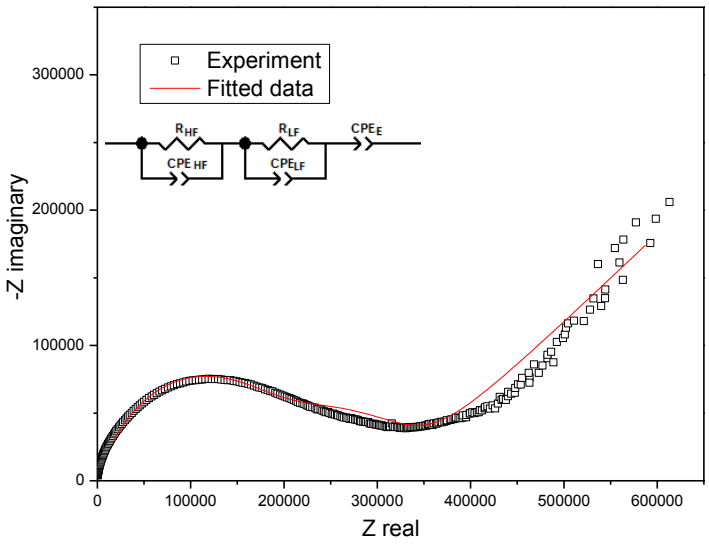

(a) room temperature impedance spectra

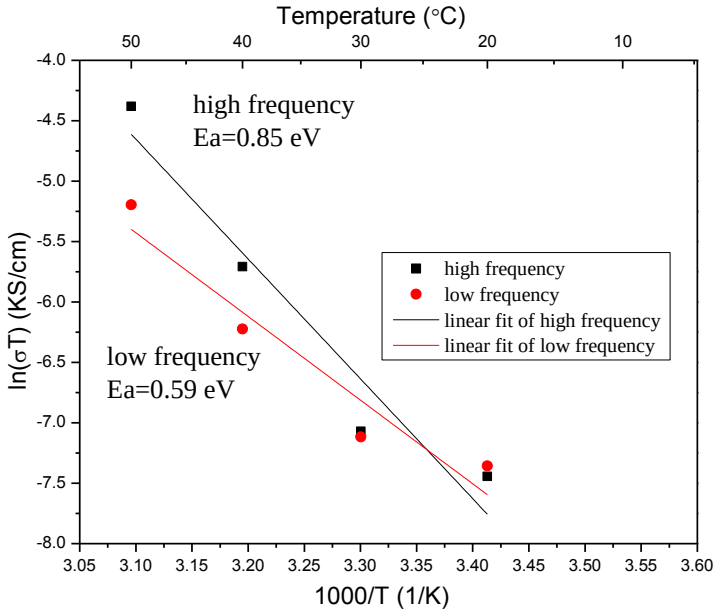

(b) Arrhenius plot

Figure 7 Ionic conductivity data of LLZTO-PEO($LiClO_4$) composite

4. CONCLUSION

$Li_{6.75}La_3Zr_{1.75}Ta_{0.25}O_{12}$ with the cubic phase garnet-type structure and porosity of about 20% was obtained by the coprecipitation method. The total conductivity at room temperature and the activation energies were estimated to be at 7.24×10^{-6} S/cm and 0.31-0.46 eV, respectively. The conductivity of the LLZTO-NASICON composite, 1.18×10^{-5} S/cm, was higher than that of LLZTO and the activation energies were estimated to be 0.23-0.58 eV. The LLZTO-PEO($LiClO_4$) composite has a similar room temperature total conductivity of 1.04×10^{-6} S/cm, but higher activation energies of 0.59-0.85 eV as compared to LLZO. This work shows the preparation and conductivity of LLZTO based composites of LLZTO-NASICON and LLZTO-PEO($LiClO_4$), which promotes the development of LLZO solid electrolyte for high safety solid-state lithium batteries.

5. ACKNOWLEDGEMENT

This work was supported primarily by NASA under award number NNX15AP44A, 2015.

6. REFERENCES

Agrawal, R.C., Pandey, G.P., 2008. Solid Polymer Electrolytes: Materials Designing and All-solid-state Battery Applications: An Overview. *Journal of Physics D: Applied Physics*, Volume 41(22), pp. 223001–223018

Allen, J.L., Wolfenstine, J., Rangasamy, E., Sakamoto, J., 2012. Effect of Substitution (Ta, Al, Ga) on the Conductivity of $Li_7La_3Zr_2O_{12}$. *Journal of Power Sources*, Volume 206, pp. 315–319

Awaka, J., Kijima, N., Hayakawa, H., Akimoto, J., 2009. Synthesis and Structure Analysis of Tetragonal $Li_7La_3Zr_2O_{12}$ with the Garnet-related Type Structure. *Journal of Solid State Chemistry*, Volume 182(8), pp. 2046–2052

Kwon, W.J., Kim, H., Jung, K., Cho, W., Kim, S.H., Lee, J., Park, M., 2017. Enhanced Li^+ Conduction in Perovskite $Li_{3x}La_{2/3-x-1/3-2x}TiO_3$ Solid-electrolytes via Microstructural Engineering. *Journal of Materials Chemistry A*., Volume 5(13), pp. 6257–6262

Liu, K., Liu, Y., Lin, D., Pei, A., Cui, Y., 2018. Materials for Lithium-ion Battery Safety. *Science Advances*, Volume 4(6), pp. 1–11

Manthiram, A., Yu, X., Wang, S., 2017. Lithium Battery Chemistries Enabled by Solid-state Electrolytes. *Nature Reviews Materials*, Volume 2, pp. 16103–16118

Morimoto, H., Awano, H., Terashima, J., Shindo, Y., Nakanishi, S., Ito, N., Ishikawa, K., Tobishima, S., 2013. Preparation of Lithium Ion Conducting Solid Electrolyte of NASICON-type $Li_{1+x}Al_xTi_{2-x}(PO_4)_3$ (x = 0.3) Obtained by using the Mechanochemical Method and Its Application as Surface Modification Materials of $LiCoO_2$ Cathode for Lithium Cell. *Journal of Power Sources*, Volume 240, pp. 636–643

Murugan, R., Thangadurai, V., Weppner, W., 2007. Fast Lithium Ion Conduction in Garnet-type Li7La $3Zr_2O_{12}$. *Angewandte Chemie - International Edition*, Volume 46(41), pp. 7778-7781

Nitta, N., Wu, F., Lee, J.T., Yushin, G., 2015. Li-ion Battery Materials: Present and Future. *Materials Today*, Volume 18(5), pp. 252–264

Reisch, M.S., 2017. Solid-state Batteries Inch Their Way toward Commercialization. *Chemical and Engineering News*, Volume 95(46), pp. 19–21

Ren, Y., Chen, K., Chen, R., Liu, T., Zhang, Y., Nan, C., 2015. Oxide Electrolytes for Lithium Batteries. *Journal of the American Ceramic Society*, Volume 98(12), pp. 3603–3623

Thangadurai, V., Narayanan, S., Pinzaru, D., 2014. Garnet-type Solid-state Fast Li Ion Conductors for Li Batteries: Critical Review. *Chemical Society Review*s, Volume 43(13), pp. 4714–4727

Varzi, A., Raccichini, R., Passerini, S., Scrosati, B., 2016. Challenges and Prospects of the Role of Solid Electrolytes in the Revitalization of Lithium Metal Batteries. *Journal of Materials Chemistry A*, Volume 4(44), pp. 17251–17259

Zhang, H., Li, C., Piszcz, M., Coya, E., Rojo, T., Rodriguez-Martinez, L., Armand, M., Zhou, Z., 2017. Single Lithium-ion Conducting Solid Polymer Electrolytes: Advances and Perspectives. *Chemical Society Reviews*, Volume 46(3), pp. 797–815

Zhao, Y., Wu, C., Peng, G., Chen, X., Yao, X., Bai, Y., Wu, F., Chen, S., Xu, X., 2016. A New Solid Polymer Electrolyte Incorporating $Li_{10}GeP_2S_{12}$ into a Polyethylene Oxide Matrix for All-solid-state Lithium Batteries. *Journal of Power Sources*, Volume 301, pp. 47–53